Вісник Тернопільського національного технічного університету
https://doi.org/10.33108/visnyk_tntu
Scientific Journal of the Ternopil National Technical University
2025, № 3 (119) https://doi.org/10.33108/visnyk_tntu2025.03
ISSN 2522-4433. Web: ***visnyk.tntu.edu.ua***

UDC 539.3

AN INTERFACE CRACK IN 1D PIEZOELECTRIC QUASICRYSTAL UNDER ANTIPLANE MECHANICAL LOADING AND ELECTRIC FIELD

Mohammed Altoumaimi; Volodymyr Loboda

Oles Honchar Dnipro National University, Dnipro, Ukraine

Abstract. *The present study considers a mode III interface crack in a one-dimensional (1D) piezoelectric quasicrystal subjected to antiplane phonon and phason loading, as well as an in-plane electric field. Due to the complex function approach, all required electromechanical parameters are presented through vector-functions analytic in the entire complex plane, except in the crack region. The cases of electrically impermeable (insulated) and electrically limited permeable conditions on the crack faces are considered. In the first case, a vector Hilbert problem in the complex plane is formulated and solved exactly. In the second case, the quadratic equation with respect to the electric flux through the crack region is also obtained. Its solution enables the determination of phonon and phason stresses, displacement jumps (sliding), and also electric characteristics along the material interface. Analytical formulas are also derived for the corresponding stress intensity factors associated with each field. Numerical computations for three selected variants of the loading conditions were conducted, and the resulting field distributions are visualised to show crack continuation beyond the crack and also inside the crack region.*

Key words: *interface crack, stress, quasicrystal, antiplane loading, limited electric permeability, problem of linear relationship*

https://doi.org/10.33108/visnyk_tntu2025.03.012 *Received 11.08.2025*

1. INTRODUCTION

Quasicrystals (QCs) are distinguished by their long-range orientation order and quasiperiodic translational symmetry, endowing them with exceptional mechanical and functional properties compared to conventional crystalline materials. The seminal discovery by Shechtman *et al.* (1984) of metallic alloys exhibiting non-periodic long-range order and high hardness stimulated extensive investigation into the elasticity and fracture behaviour of these materials [1].

The foundational continuum theory of QC elasticity incorporates coupled phonon and phason displacement fields. In pioneering work, Ding *et al.* (1993) formulated the generalized elastic constitutive relations for quasicrystals, deriving the full electro-elastic coupling between phonon and phason modes [2]. Building on this framework, Fan (2011) provided a comprehensive mathematical treatment of QC elasticity and its applications, including explicit solutions for fundamental boundary-value problems [3]. Fracture mechanics of QCs under anti-plane shear (Mode III) has been addressed in several studies. Shi *et al.* (2007) analysed interfacial cracks between conventional elastic materials and quasicrystals, highlighting the role of phason fields in crack tip stress singularities [4]. Zhou and Li (2018) derived exact solutions for two collinear cracks normal to a 1D hexagonal piezoelectric QC boundary, obtaining closed-form expressions for stress intensity factors and displacement fields [5].

A non-uniformly loaded anti-plane crack embedded in a half-space of a one-dimensional piezoelectric quasicrystal was studied in [6], and two collinear electrically permeable anti-plane cracks of equal length lying at the mid-plane of a one-dimensional

hexagonal piezoelectric quasicrystal strip were investigated in [7]. Two thin strips with a microcrack at the interface were studied in paper [8]. Piezoelectric coupling in QCs introduces additional complexity. Hu *et al.* (2019) reduced the mixed electro-mechanical boundary-value problem for an interface crack in dissimilar 1D hexagonal piezoelectric QCs to singular integral equations via Riemann-Hilbert methods, yielding full-field solutions for phonon, phason, and electric quantities along the crack faces [9]. Govorukha and Kamlah (2024) extended these results by considering mixed electric boundary conditions, combining conducting and permeable crack face segments, demonstrating how partial electrical contact modulates crack-tip intensity factors [10]. Loboda et al. further generalized to multiple collinear interface cracks in layered piezoelectric QCs, revealing interaction effects on stress intensity factors and energy release rates under coupled electromechanical loading [11].

An electrically limited permeable interface crack model was proposed by Hao and Shen [12] for the plane problem of a homogeneous piezoelectric material. To date, an exact anti-plane analytical solution for an electrically limited permeable interface crack between dissimilar piezoelectric QCs has not been presented. The present study addresses this gap by (i) formulating the coupled phonon-phason-electric field equations for a bimaterial QC plate, (ii) reducing the interface crack boundary-value problem to a vector Hilbert problem, (iii) deriving closed-form expressions for crack-face opening displacement and electric potential jump, and (iv) obtaining analytical formulas for the stress intensity factors associated with each field. Numerical validation and visualization of field distributions in the crack-continuation region complete the solution, offering a practical tool for design and optimization of QC-based electromechanical systems.

2. FORMULATION OF THE BASIC RELATIONS

For the linear elastic theory of QCs, the constitutive relations, equilibrium equations and geometric equations of a 1D piezoelectric hexagonal QC with point group 6 *mm* without body forces and free charges can be expressed in the following form [13]

$$\sigma_{ij} = c_{ijks}\varepsilon_{ks} - e_{sij}E_s + R_{ij3s}w_{3s}\,, \tag{1}$$

$$D_i = e_{iks}\varepsilon_{ks} + \xi_{is}E_s + \hat{e}_{i3s}w_{3s}\,, \tag{2}$$

$$H_{3i} = R_{ks3i}\varepsilon_{ks} - \hat{e}_{s3i}E_s + K_{3i3s}w_{3s}\,, \tag{3}$$

$$\sigma_{ij,j} = 0\,,\ D_{i,i} = 0\,,\ H_{3i,i} = 0\,, \tag{4}$$

$$\varepsilon_{ij} = \tfrac{1}{2}(u_{i,j} + u_{j,i})\,,\ E_i = -\phi_{,i}\,,\ w_{3i} = w_{3,i}\,, \tag{5}$$

where $i, j, k, s = 1, 2, 3$, and the denotation, represents the derivative operation for the space variables;

u_i, w_3 and φ are the phonon displacements, phason displacement, and electric potential, respectively, and the atom arrangement is periodic in the $x_1 - x_2$ plane and quasi-periodic in the x_3 -axis;

σ_{ij} and ε_{ks} are the phonon stresses and strains, respectively; H_{3i} and w_{3i} are the phason stresses and strains, respectively;

D_i and E_i are the electric displacements and electric fields, respectively, and the polarization direction is along the x_3 -axis;

c_{ijks} and K_{3j3s} are the elastic constants in the phonon and phason fields, respectively;

R_{ij3k} represent the phonon–phason coupling elastic constants;

e_{jks} and $\hat{e}_{jks}$ are the piezoelectric constants in the phonon and phason fields, respectively;

ξ_{is} are the permittivity constants.

Here, a comma in subscript denotes differentiation with respect to the following spatial variable.

For the case of antiplane mechanical loading and an in-plane electric loading with reference to the x_1Ox_2-plane all fields are independent of the variable x_3. Therefore, the problem under consideration is a so-called anti-plane shear problem or mode-III crack problem. In this case

$$u_1 = u_2 = 0,\ u_3 = u_3\left(x_1, x_2\right),\ w_3 = w_3\left(x_1, x_2\right),\ \varphi = \varphi\left(x_1, x_2\right), \tag{6}$$

and the constitutive relations take the form:

$$\begin{Bmatrix} \sigma_{j3} \\ H_{j3} \\ D_j \end{Bmatrix} = \mathbf{R} \begin{Bmatrix} u_{3,j} \\ w_{3,j} \\ \varphi_{,j} \end{Bmatrix} \ \left(j = 1,2\right), \tag{7}$$

where

$$\mathbf{R} = \begin{bmatrix} c_{44} & R_3 & e_{15} \\ R_3 & K_2 & \hat{e}_{15} \\ e_{15} & \hat{e}_{15} & -\xi_{11} \end{bmatrix}, \tag{8}$$

and c_{44}, K_2, R_3 stand for the phonon elastic modulus, phason elastic modulus and phonon-phason coupling modulus, respectively, which are written in the simplified index notation. Also e_{15}, $\hat{e}_{15}$ are the piezoelectric constants of the phonon and phason fields and ξ_{11} is the permittivity. Introducing the vectors

$$\boldsymbol{u} = \left[u_3, w_3, \varphi\right]^T,\ \boldsymbol{t}_j = \left[\sigma_{3j}, H_{3j}, D_j\right]^T, \tag{9}$$

one can write

$$\boldsymbol{t}_j = \boldsymbol{R}\boldsymbol{u}_{,j} \ \left(j = 1,2\right). \tag{10}$$

For the considered anti-plane problem, the equilibrium equations (4) take the form

$$\frac{\partial \sigma_{31}}{\partial x_1} + \frac{\partial \sigma_{32}}{\partial x_2} = 0,\ \frac{\partial D_1}{\partial x_1} + \frac{\partial D_2}{\partial x_2} = 0,\ \frac{\partial H_{31}}{\partial x_1} + \frac{\partial H_{32}}{\partial x_2} = 0.$$

Substituting (7) in the last equation, we get that the functions u_3, φ and w_3 satisfy the equations $\Delta u_3 = 0$, $\Delta\varphi = 0$, $\Delta w_3 = 0$, respectively, i.e. they are harmonic. Therefore, present the vector $\boldsymbol{u}$, composed of these functions, as real parts of some analytic vector-function

$$\boldsymbol{u} = 2\,\mathrm{Re}\boldsymbol{\Phi}(z) = \boldsymbol{\Phi}(z) + \bar{\boldsymbol{\Phi}}(\bar{z}) \text{ (2 is introduced for convenience),} \tag{11}$$

where $\boldsymbol{\Phi}(z) = \left[\Phi_1(z), \Phi_2(z), \Phi_3(z)\right]^T$ is an arbitrary analytic vector-function of the complex variable $z = x_1 + ix_2$.

Substituting (11) in (10), one gets

$$\boldsymbol{t}_1 = -i\boldsymbol{B}\boldsymbol{\Phi}'(z) + i\bar{\boldsymbol{B}}\bar{\boldsymbol{\Phi}}'(\bar{z}),\ \boldsymbol{t}_2 = \boldsymbol{B}\boldsymbol{\Phi}'(z) + \bar{\boldsymbol{B}}\bar{\boldsymbol{\Phi}}'(\bar{z}), \tag{12}$$

where $\boldsymbol{B} = i\boldsymbol{R}$.

Bimaterial plane. Suppose that the plane (x_1, x_2) is composed of two half-planes $x_2 > 0$ and $x_2 < 0$. Different cracks, inclusions and other defects can take place on the axis x_1. The presentation (11), (12) can be written for regions $x_2 > 0$ and $x_2 < 0$ which in this case takes the form

$$\boldsymbol{u}^{(m)} = \boldsymbol{\Phi}^{(m)}(z) + \bar{\boldsymbol{\Phi}}^{(m)}(\bar{z}),\quad \boldsymbol{t}_2^{(m)} = \boldsymbol{B}^{(m)}\boldsymbol{\Phi}'^{(m)}(z) + \bar{\boldsymbol{B}}^{(m)}\bar{\boldsymbol{\Phi}}'^{(m)}(\bar{z}), \tag{13}$$

where $m = 1$ for area 1 and $m = 2$ for the area 2;
$\boldsymbol{B}^{(m)}$ are the matrices $\boldsymbol{B}$ for areas 1 and 2, respectively;
$\boldsymbol{\Phi}^{(m)}(z)$ are the arbitrary vector functions, analytic in the areas 1 and 2, respectively.

Next, we require that the equality $\boldsymbol{t}_2^{(1)} = \boldsymbol{t}_2^{(2)}$ holds true on the entire axis x_1. Then it follows from (13)

$$\boldsymbol{B}^{(1)}\boldsymbol{\Phi}'^{(1)}(x_1 + i0) + \bar{\boldsymbol{B}}^{(1)}\bar{\boldsymbol{\Phi}}'^{(1)}(x_1 - i0) = \boldsymbol{B}^{(2)}\boldsymbol{\Phi}'^{(2)}(x_1 - i0) + \bar{\boldsymbol{B}}^{(2)}\bar{\boldsymbol{\Phi}}'^{(2)}(x_1 + i0). \tag{14}$$

Here, we have used the first form of designation $F(x_1 \pm i0) = F^{\pm}(x_1)$, which refers to the limit value of a function $F(z)$ at $y \to 0$ from above or below, respectively.

The equation (14) can be written as

$$\boldsymbol{B}^{(1)}\boldsymbol{\Phi}'^{(1)}(x_1 + i0) - \bar{\boldsymbol{B}}^{(2)}\bar{\boldsymbol{\Phi}}'^{(2)}(x_1 + i0) = \boldsymbol{B}^{(2)}\boldsymbol{\Phi}'^{(2)}(x_1 - i0) - \bar{\boldsymbol{B}}^{(1)}\bar{\boldsymbol{\Phi}}'^{(1)}(x_1 - i0).$$

The left and right sides of the last equation can be considered as the boundary values of the functions

$$\boldsymbol{B}^{(1)}\boldsymbol{\Phi}'^{(1)}(z) - \bar{\boldsymbol{B}}^{(2)}\bar{\boldsymbol{\Phi}}'^{(2)}(z) \text{ and } \boldsymbol{B}^{(2)}\boldsymbol{\Phi}'^{(2)}(z) - \bar{\boldsymbol{B}}^{(1)}\bar{\boldsymbol{\Phi}}'^{(1)}(z), \tag{15}$$

which are analytic in the upper and lower planes, respectively. But it means that there is a function $\mathbf{M}(z)$, which is equal to the mentioned functions in each half-plane and is analytic in the entire plane. This function is the following:

$$\mathbf{M}(z) = \begin{cases} \boldsymbol{B}^{(1)}\boldsymbol{\Phi}'^{(1)}(z) - \bar{\boldsymbol{B}}^{(2)}\bar{\boldsymbol{\Phi}}'^{(2)}(z) & \text{for } x_2 > 0 \\ \boldsymbol{B}^{(2)}\boldsymbol{\Phi}'^{(2)}(z) - \bar{\boldsymbol{B}}^{(1)}\bar{\boldsymbol{\Phi}}'^{(1)}(z) & \text{for } x_2 < 0 \end{cases}$$

Assuming that $\mathbf{M}(z)\big|_{z\to\infty}\to 0$, on the basis of the Liouville theorem, we find that each of the functions (15) is equal to 0 for each z from the corresponding half-plane. Hence, we obtain

$$\bar{\boldsymbol{\Phi}}'^{(2)}(z)=\left(\bar{\boldsymbol{B}}^{(2)}\right)^{-1}\boldsymbol{B}^{(1)}\boldsymbol{\Phi}'^{(1)}(z)\ \text{ for }\ x_2>0, \tag{16}$$

$$\bar{\boldsymbol{\Phi}}'^{(1)}(z)=\left(\bar{\boldsymbol{B}}^{(1)}\right)^{-1}\boldsymbol{B}^{(2)}\boldsymbol{\Phi}'^{(2)}(z)\ \text{ for }\ x_2<0. \tag{17}$$

Further, we find the jump of the following vector-function

$$\left\langle \boldsymbol{u}'(x_1)\right\rangle=\boldsymbol{u}'^{(1)}\left(x_1+i0\right)-\boldsymbol{u}'^{(2)}\left(x_1-i0\right), \tag{18}$$

when passing through the interface. Finding from the first formula (13)

$$\boldsymbol{u}'^{(m)}\left(z\right)=\boldsymbol{\Phi}'^{(m)}(z)+\bar{\boldsymbol{\Phi}}'^{(m)}(\bar{z})$$

or

$$\boldsymbol{u}'^{(m)}\left(x_1\pm i0\right)=\boldsymbol{\Phi}'^{(m)}\left(x_1\pm i0\right)+\bar{\boldsymbol{\Phi}}'^{(m)}\left(x_1\mp i0\right)$$

and substituting in (18), one gets

$$\left\langle \boldsymbol{u}'(x_1)\right\rangle=\boldsymbol{\Phi}'^{(1)}\left(x_1+i0\right)+\bar{\boldsymbol{\Phi}}'^{(1)}\left(x_1-i0\right)-\boldsymbol{\Phi}'^{(2)}\left(x_1-i0\right)-\bar{\boldsymbol{\Phi}}'^{(2)}\left(x_1+i0\right).$$

Finding further of (17) $\boldsymbol{\Phi}'^{(2)}\left(x_1-i0\right)=\left(\boldsymbol{B}^{(2)}\right)^{-1}\bar{\boldsymbol{B}}^{(1)}\bar{\boldsymbol{\Phi}}'^{(1)}\left(x_1-i0\right)$ and substituting this expression together with (16), at $x_2\to+0$, in the latest formula, leads to

$$\left\langle \boldsymbol{u}'(x_1)\right\rangle=\boldsymbol{D}\boldsymbol{\Phi}'^{(1)}\left(x_1+i0\right)+\bar{\boldsymbol{D}}\bar{\boldsymbol{\Phi}}'^{(1)}\left(x_1-i0\right),$$

where $\boldsymbol{D}=\mathbf{I}-\left(\bar{\boldsymbol{B}}^{(2)}\right)^{-1}\boldsymbol{B}^{(1)}$, $\boldsymbol{I}=diag\left[1,1,1\right]$ – the identity matrix.

Introducing a new vector-function

$$\boldsymbol{W}\left(z\right)=\begin{cases}\boldsymbol{D}\boldsymbol{\Phi}'^{(1)}\left(z\right), & x_2>0\\ -\bar{\boldsymbol{D}}\bar{\boldsymbol{\Phi}}'^{(1)}\left(z\right), & x_2<0\end{cases}, \tag{19}$$

the expression for the derivative of the displacement jump can be written as

$$\left\langle \mathbf{u}'\left(x_1\right)\right\rangle=\boldsymbol{W}^{+}\left(x_1\right)-\boldsymbol{W}^{-}\left(x_1\right). \tag{20}$$

From the second relation (13), we have

$$\boldsymbol{t}_2^{(1)}\left(x_1,0\right)=\boldsymbol{B}^{(1)}\boldsymbol{\Phi}'^{(1)}\left(x_1+i0\right)+\bar{\boldsymbol{B}}^{(1)}\bar{\boldsymbol{\Phi}}'^{(1)}\left(x_1-i0\right). \tag{21}$$

Given that on the basis of (19)

$$\boldsymbol{\Phi}'^{(1)}\left(x_1+i0\right)=\boldsymbol{D}^{-1}\boldsymbol{W}\left(x_1+i0\right),$$

$$\bar{\boldsymbol{\Phi}}'^{(1)}(x_1 - i0) = -\left(\bar{\boldsymbol{D}}^{-1}\right)^{-1} \boldsymbol{W}(x_1 - i0)$$

and substituting these relations in (21) leads to

$$\boldsymbol{t}_2^{(1)}(x_1, 0) = \boldsymbol{G}\boldsymbol{W}^{+}(x_1) - \bar{\mathbf{G}}\boldsymbol{W}^{-}(x_1), \tag{22}$$

where $\boldsymbol{G} = \boldsymbol{B}^{(1)}\boldsymbol{D}^{-1}$. Simple calculations show that

$$\boldsymbol{G} = \left[\left(\boldsymbol{B}^{(1)}\right)^{-1} + \left(\boldsymbol{B}^{(2)}\right)^{-1}\right]^{-1}, \tag{23}$$

moreover, $\bar{\boldsymbol{G}} = -\boldsymbol{G}$. Then the equation (22) takes the form

$$\boldsymbol{t}_2^{(1)}(x_1, 0) = \boldsymbol{G}\left(\boldsymbol{W}^{+}(x_1) + \boldsymbol{W}^{-}(x_1)\right). \tag{24}$$

The representations (20) and (24) are very convenient for solving antiplane problems for bimaterial piezoelectric QCs with cracks and inclusions at the interface.

3. AN ELECTRICALLY INSULATED CRACK BETWEEN TWO PIEZOELECTRIC QUASICRYSTALS

Consider a crack $|x_1| < a$ with mechanically free and electrically-insulated faces at the interface $x_2 = 0$ (fig. 1).

The shear phonon σ_{32}^{∞} and phason H_{32}^{∞} stresses and electric flux are prescribed at infinity and are designated by the vector $\boldsymbol{t}_2^{\infty} = \left[\sigma_{32}^{\infty}, H_{32}^{\infty}, D_2^{\infty}\right]$.

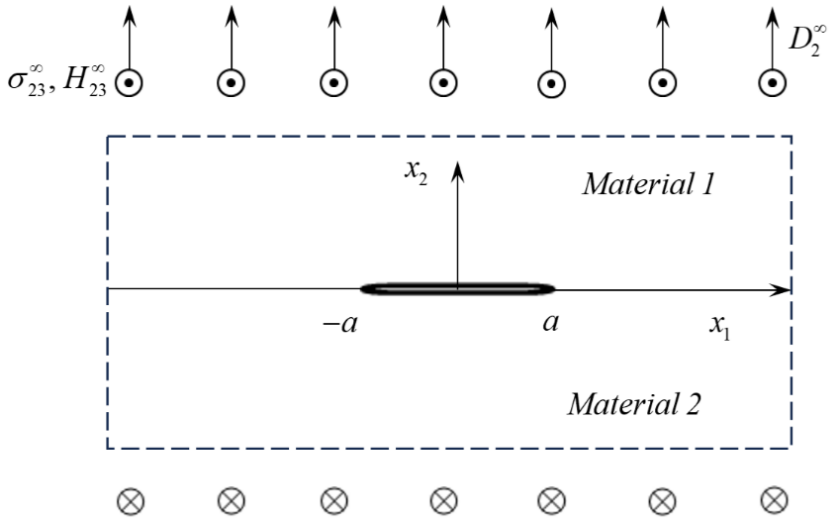

Figure 1. The crack between two piezoelectric quasicrystals

The boundary conditions at the interface are of the form

$$\sigma_{32}^{(1)} = \sigma_{32}^{(2)} = 0,\ D_2^{(1)} = D_2^{(2)} = 0,\ H_{32}^{(1)} = H_{32}^{(2)} = 0 \ \text{ for } |x_1| < a, \tag{25}$$

$$\langle \sigma_{32} \rangle = 0, \langle D_2 \rangle = 0, \langle H_{32} \rangle = 0, \langle \varepsilon_{31} \rangle = 0, \langle E_1 \rangle = 0, \langle w_{31} \rangle = 0 \quad \text{for } |x_1| > a, \tag{26}$$

where $\langle * \rangle$ means a jump of the corresponding function when passing through the axis x_1.

The first three conditions (26) are satisfied based on (14). From the satisfaction of the last three conditions (26), the analyticity of the vector function $\boldsymbol{W}(z)$ in the whole plane, except for the crack area, follows due to (20). Also, the fulfilment of the conditions (25) using (24) leads to the vector Hilbert problem of linear relationship

$$\boldsymbol{W}^+(x_1) + \boldsymbol{W}^-(x_1) = 0 \text{ for } x_1 \in (-a, a). \tag{27}$$

Taking into account that $\boldsymbol{W}^+(x_1) = \boldsymbol{W}^-(x_1) = \boldsymbol{W}(x_1)$ for $x_1 \notin (-a, a)$ and $\boldsymbol{W}(x_1)\big|_{x_1 \to \infty} = \boldsymbol{W}(z)\big|_{z \to \infty}$ we get by using (24) the following condition at infinity

$$\boldsymbol{W}(z)\big|_{z \to \infty} = \frac{1}{2} \boldsymbol{G}^{-1} \boldsymbol{t}_2^{\infty}. \tag{28}$$

The solution of the problem (27) under the condition at infinity (28) has the form [14]

$$\boldsymbol{W}(z) = \frac{1}{2} \boldsymbol{G}^{-1} \boldsymbol{t}_2^{\infty} \frac{z}{\sqrt{z^2 - a^2}}. \tag{29}$$

Substituting (29) in (24), we obtain:

$$\boldsymbol{t}_2^{(1)}(x_1, 0) = \boldsymbol{t}_2^{\infty} \frac{x_1}{\sqrt{x_1^2 - a^2}} \text{ for } x_1 \notin [-a, a]. \tag{30}$$

Considering that $\boldsymbol{W}^-(x_1) = -\boldsymbol{W}^+(x_1) = \boldsymbol{W}(x_1)$ for $x_1 \in (-a, a)$, one gets from relations (20), (29)

$$\langle \mathbf{u}'(x_1) \rangle = \boldsymbol{G}^{-1} \boldsymbol{t}_2^{\infty} \frac{x_1}{i\sqrt{a^2 - x_1^2}} \text{ for } x_1 \in (-a, a). \tag{31}$$

Integrating the last relation leads to the following formula for the jump in displacement of the crack faces

$$\langle \mathbf{u}(x_1) \rangle = i \boldsymbol{G}^{-1} \boldsymbol{t}_2^{\infty} \sqrt{a^2 - x_1^2}. \tag{32}$$

4. THE CASE OF PRESCRIBED ELECTRICAL DISPLACEMENTS AT THE CRACK FACES

Let's assume that a nonzero electric displacement $D_2^{(1)} = D_2^{(2)} = D_0$ is prescribed at the crack faces. In this case, one has in the crack region:

$$\boldsymbol{t}_2^{(1)}(x_1, 0) = \boldsymbol{t}_2^{(0)} \text{ for } x_1 \in (-a, a)$$

where $\boldsymbol{t}_2^{(0)} = \{0, 0, D_0\}^T$

Then, from the last equation and (24), we have

$$\boldsymbol{W}^{+}\left(x_1\right)+\boldsymbol{W}^{-}\left(x_1\right)=\boldsymbol{G}^{-1}\mathbf{t}_2^{(0)} \text{ for } x_1\in\left(-a,a\right) \tag{33}$$

Introducing a new vector-function $\mathbf{Y}(z)$ by means of the formula

$$\boldsymbol{W}\left(z\right)=\mathbf{Y}(z)+\frac{1}{2}\boldsymbol{G}^{-1}\mathbf{t}_2^{(0)}, \tag{34}$$

we get from (33):

$$\mathbf{Y}^{+}\left(x_1\right)+\mathbf{Y}^{-}\left(x_1\right)=0 \text{ for } x_1\in\left(-a,a\right). \tag{35}$$

Condition at infinity (28) transforms into the form

$$\mathbf{Y}\left(z\right)\big|_{z\to\infty}=\frac{1}{2}\boldsymbol{G}^{-1}\left(\boldsymbol{t}_2^{\infty}-\mathbf{t}_2^{(0)}\right). \tag{36}$$

The solution of the problem (35), (36) takes the form:

$$\mathbf{Y}\left(z\right)=\frac{1}{2}\boldsymbol{G}^{-1}\left(\boldsymbol{t}_2^{\infty}-\boldsymbol{t}_2^{(0)}\right)\frac{z}{\sqrt{z^2-a^2}} \tag{37}$$

Using further (24), (34) and (37), we get

$$\boldsymbol{t}_2^{(1)}\left(x_1,0\right)=\boldsymbol{G}\left(\mathbf{Y}^{+}\left(x_1\right)+\mathbf{Y}^{-}\left(x_1\right)\right)+\mathbf{t}_2^{(0)},$$

Taking into account that $\mathbf{Y}^{+}\left(x_1\right)=\mathbf{Y}^{-}\left(x_1\right)=\mathbf{Y}\left(x_1\right)$ for $x_1\notin\left(-a,a\right)$ one obtains

$$\boldsymbol{t}_2^{(1)}\left(x_1,0\right)=2\boldsymbol{G}\,\mathbf{Y}\left(x_1\right)+\mathbf{t}_2^{(0)}=\left(\boldsymbol{t}_2^{\infty}-\boldsymbol{t}_2^{(0)}\right)\frac{z}{\sqrt{z^2-a^2}}+\mathbf{t}_2^{(0)} \text{ for } x_1\notin\left(-a,a\right). \tag{38}$$

Equation (38) in the complete form can be written as

$$\sigma_{23}\left(x_1,0\right)=\sigma_{32}^{\infty}\frac{z}{\sqrt{z^2-a^2}},\ H_{23}\left(x_1,0\right)=H_{32}^{\infty}\frac{z}{\sqrt{z^2-a^2}},\ D_2\left(x_1,0\right)=\left(D_2^{\infty}-D_0\right)\frac{z}{\sqrt{z^2-a^2}}+D_0 \tag{39}$$

The stress and electric displacement intensity factors (SIF) at the point a can be introduced in the following vector form:

$$\mathbf{K}=\lim_{x_1\to a-0}\sqrt{2\pi(x_1-a)}\,\boldsymbol{t}_2^{(1)}\left(x_1,0\right), \tag{40}$$

where $\mathbf{K}=\left[K_{3\sigma},K_{3H},K_D\right]^T$

Substituting the expressions (38), (39) into (40), we get

$$K_{3\sigma}=\sqrt{\pi a}\sigma_{32}^{\infty},\ K_{3H}=\sqrt{\pi a}H_{32}^{\infty},\ K_D=\sqrt{\pi a}\left(D_2^{\infty}-D_0\right) \tag{41}$$

On the basis of (20), (34) and (35), we arrive at the formula

$$\left\langle \mathbf{u}'(x_1) \right\rangle = \boldsymbol{G}^{-1}\left(\boldsymbol{t}_2^{\infty} - \boldsymbol{t}_2^{(0)}\right)\frac{x_1}{i\sqrt{a^2 - x_1^2}} \text{ for } x_1 \in (-a, a), \tag{42}$$

which gives after integration

$$\left\langle \mathbf{u}(x_1) \right\rangle = i\boldsymbol{G}^{-1}\left(\boldsymbol{t}_2^{\infty} - \boldsymbol{t}_2^{(0)}\right)\sqrt{a^2 - x_1^2} \text{ for } x_1 \in (-a, a). \tag{43}$$

Expression (43) in the complete form is the following

$$\begin{Bmatrix} \langle u_3 \rangle \\ \langle w_3 \rangle \\ \langle \varphi \rangle \end{Bmatrix} = \mathbf{M} \begin{Bmatrix} \sigma_{32}^{\infty} \\ H_{32}^{\infty} \\ D_2^{\infty} - D_0 \end{Bmatrix} \sqrt{a^2 - x_1^2} \tag{44}$$

where $\mathbf{M} = i\mathbf{G}^{-1}$.

5. ELECTRICALLY LIMITED PERMEABLE CRACK

Consider now another crack model in which the relation between the electric potential and displacement jumps along the crack region is taken into account. We assume now that the crack filler has the dielectric permittivity

$$\varepsilon_a = \varepsilon_r \varepsilon_0,$$

where ε_r is the relative dielectric permittivity and $\varepsilon_0 = 8.85 \times 10^{-12} C/Vm$ is the dielectric constant of a vacuum. We also assume that the crack faces are free of prescribed mechanical loading and electric charges. Moreover, similarly to [12], we consider that the electric field inside the crack can be found as

$$E_a = -\frac{\varphi^+ - \varphi^-}{u_3^+ - u_3^-} \text{ for } x_1 \in (-a, a).$$

where the superscripts «+» and «–» indicate the upper and lower faces of the interface, respectively.

Taking into account that $D_2 = \varepsilon_a E_a$ and designating D_2 at the crack faces as D_0, one arrives at the following electric condition

$$D_0 = -\varepsilon_a \frac{\varphi^+ - \varphi^-}{u_3^+ - u_3^-} = -\varepsilon_a \frac{\langle \varphi \rangle}{\langle u_3 \rangle} \text{ for } x_1 \in (-a, a) \tag{45}$$

along the crack region. It is worth mentioning that we use the same designation for the electric displacement on the crack faces as in the previous section, but in this case D_0 is unknown and should be found from Eq. (45).

Taking into account that Eq. (44) remains valid in this case, Eq. (45) can be written in the following form

$$D_0 = -\varepsilon_a \frac{M_{31}\sigma_{32}^{\infty} + M_{32}H_{32}^{\infty} + M_{33}\left(D_2^{\infty} - D_0\right)}{M_{11}\sigma_{32}^{\infty} + M_{12}H_{32}^{\infty} + M_{13}\left(D_2^{\infty} - D_0\right)} \tag{46}$$

Equation (46) represents the quadratic equation with respect to the electric displacement D_0. After simplification, it can be written as

$$D_0^2 - \chi_1 D_0 - \chi_2 = 0 \tag{47}$$

where

$$\chi_1 = \left(M_{11}\sigma_{32}^{\infty} + M_{12}H_{32}^{\infty} + M_{13}D_2^{\infty} - \varepsilon_a\right)/M_{13},\ \chi_2 = \varepsilon_a\left(M_{31}\sigma_{32}^{\infty} + M_{32}H_{32}^{\infty} + M_{33}D_2^{\infty}\right)/M_{13}$$

The analysis of the solution of Eq. (47) shows that one of the two roots is physically unacceptable; therefore, in the following, we'll pay our attention only to the physically acceptable root of this equation.

6. NUMERICAL ILLUSTRATION AND DISCUSSION

In this section, the main attention will be devoted to the electrically limited permeable crack model, which best reflects the physical peculiarities of the crack deformation. Consider for the analysis the piezoelectric QCs with the following values of the required parameters [15, 16]:
$c_{44}^{(1)} = 5.0\times10^{10}\,Pa$, $e_{15}^{(1)} = -0.318\,C/m^2$, $K_2^{(1)} = 0.3\times10^{9}\,Pa$, $R_3^{(1)} = 1.2\times10^{9}\,Pa$,
$\hat{e}_{15}^{(1)} = -0.16\,C/m^2$, $\xi_{11}^{(1)} = 8.25\times10^{-11}\,C^2/(Nm^2)$ for the upper material,
$c_{44}^{(2)} = 3.55\times10^{10}\,Pa$, $e_{15}^{(2)} = 17\,C/m^2$, $K_2^{(2)} = 0.15\times10^{9}\,Pa$, $R_3^{(2)} = 1.765\times10^{9}\,Pa$,
$\hat{e}_{15}^{(2)} = 17\,C/m^2$, $\xi_{11}^{(2)} = 15.1\times10^{-9}\,C^2/(Nm^2)$ for the lower one.

It is worth mentioning that the matrix $\mathbf{M}$ in this case is the following

$$\mathbf{M} = \begin{bmatrix} 5.3090\times10^{-11} & -9.8852\times10^{-11} & 0.03892 \\ -9.8852\times10^{-11} & -1.9204\times10^{-9} & -3.2408 \\ 0.03892 & -3.2408 & -5.8781\times10^{9} \end{bmatrix}.$$

For the illustration, we'll choose $a = 0.01\ m$ and the cases of the external loading given in Table 1. In the last column of this Table, the corresponding values of electric flux D_0, obtained from Eq. (47), are given.

Table 1

Load cases and corresponding electric flux D_0

Case	$10^{-6}\sigma_{32}^{\infty}$ [Pa]	$10^{-6}H_{32}^{\infty}$ [Pa]	$100D_2^{\infty}$ [C/m^2]	$100D_0$ [C/m^2]
Case 1	6.0	7.0	0.5	0.9506
Case 2	8.0	9.0	0.75	1.1982
Case 3	10.0	11.0	1.0	1.5651

It is evident from Table 1 that relatively close values of external loading result in significantly different magnitudes of the electric flux through the crack region.

The graphs of phonon, phason and electric quantities along the material interface are given in Figures 2–4. Particularly phonon shear stress $\sigma_{32}(x_1,0)$ [Pa] at the right crack continuation and the phonon crack faces jump (crack sliding) $\langle u_3(x_1)\rangle$ [m] are shown in Fig. 2 (a) and (b), respectively. Here and in the following figures, the solid, dashed, and dotted lines represent cases 1, 2, and 3, respectively.

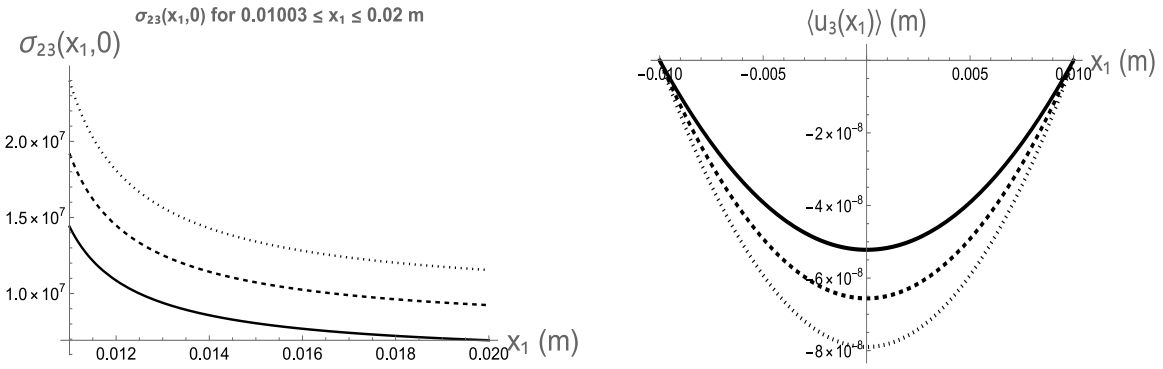

(a) (b)

Figure 2. Phonon shear stress at the right crack continuation (a) and the phonon crack faces jump (b) for three cases of the loading

Phason stress $H_{32}(x_1,0)$ [Pa] at the right crack continuation and the phason crack faces jump $\langle w_3(x_1)\rangle$ [m] are shown in Fig. 3 (a) and (b), respectively.

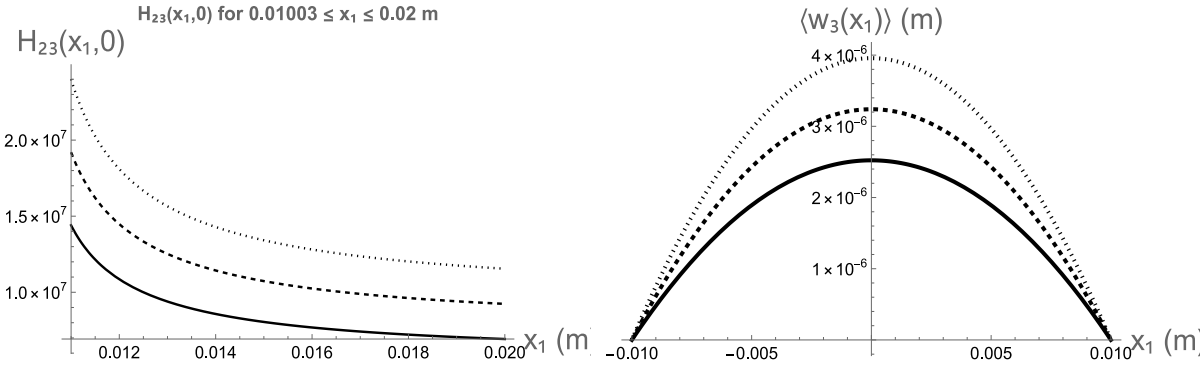

(a) (b)

Figure 3. Phason stress at the right crack continuation (a) and the phonon crack faces jump (b)

The electric displacement $D_2(x_1,0)$ [C/m^2] at the right crack continuation and the electric field jump over the crack faces $\langle \varphi(x_1)\rangle$ [V] are shown in Fig. 4 (a) and (b), respectively.

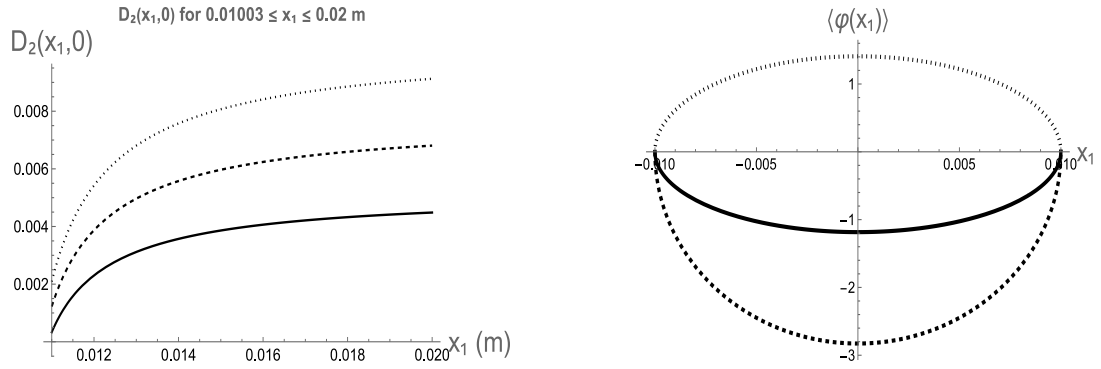

(a) (b)

Figure 4. Electric displacement at the right crack continuation and the electric field jump through the crack faces

As can be seen from formulas (38) and (39), phonon and phason stresses, as well as the electric displacement, exhibit a square root singularity at the crack tips. For this reason, their graphs in Figures 2 (a), 3 (a), and 4 (a) are drawn only in the interval (0.01003 m <x1< 0.02 m), i.e. at some distance from the crack tip.

The SIFs for the three selected cases of loading were calculated using the formulas (41) and are presented in Table 2.

Table 2

Stress Intensity Factors (SIF) for three selected cases

Case	$K_{3\sigma}$ [Pa√m]	K_{3H} [Pa√m]	K_D [C $m^{3/2}$]
Case 1	1.504×10^7	1.755×10^7	0.02211
Case 2	2.005×10^7	2.256×10^7	0.03110
Case 3	2.507×10^7	2.757×10^7	0.04010

7. CONCLUSIONS

A Mode III interface crack in a one-dimensional quasicrystal with piezoelectric effect is considered under anti-plane mechanical and in-plane electric loading. The complex function method was used, and all electromechanical parameters are presented through vector-functions that are analytic in the entire complex plane, except in the crack region, as given by Equations (20) and (24). Electrically impermeable and electrically limited permeable crack models are assumed for analysis. The first case leads to the vector Hilbert problem (27) with the condition at infinity (28), and the second one requires the additional solution of the quadratic equation (47) with respect to the electric flux through the crack region. The case of a nonzero prescribed electric displacement on the crack faces is also considered in Section 4. For all considered types of electrical conditions, analytical formulas for phonon and phason stresses, displacement jumps, electric components along the material interface, and the corresponding stress intensity factors at the crack tip are derived.

Three variants of the loading given in Table 1 were chosen for the numerical illustration. The corresponding values of electric flux D_0 are also given in this table. Other numerical results

are summarised in Figures 2–4 and Table 2. Particularly, phonon shear stress $\sigma_{32}(x_1,0)$, phason stress $H_{32}(x_1,0)$ and the electric displacement $D_2(x_1,0)$ along the right crack continuation are given in Figures 2 (a) – 4 (a), respectively. Phonon $\langle u_3(x_1)\rangle$ and phason $\langle w_3(x_1)\rangle$ crack faces displacement jumps are shown in Figures 2 (b) and 3 (b), respectively, and the electric potential jump is given in Fig. 4 (b). It follows from the obtained results that along the crack-continuation region beyond the crack, the phonon and phason shear stresses decay proportionally to the inverse square root of the distance from the tip, whereas the electric displacement converges more gradually to its remote value. Besides, rather close values of external loading lead to very different magnitudes of the electric flux through the crack region, and both kinds of crack faces displacement and electric potential jumps maintain the square root parabolic behavior along the crack region.

References

1. Shechtman D., Blech I., Gratias D., Cahn J. W. (1984) Metallic phase with long-range orientational order and no translational symmetry. *Phys. Rev. Lett.*, 53, pp. 1951–1953. https://doi.org/10.1103/PhysRevLett.53.1951
2. Ding D. H., Yang W., Hu C. Z., Wang R. (1993) Generalized elasticity theory of quasicrystals. *Phys. Rev. B*, 48, pp. 7003–7010. https://doi.org/10.1103/PhysRevB.48.7003
3. Fan T. Y. (2011). *Theory of Elasticity of Quasicrystals and Its Applications.* Springer. https://doi.org/10.1007/978-3-642-14643-5
4. Shi W. C., Li H. H., Gao Q. H. (2007) Interfacial cracks of antiplane sliding mode between usual elastic materials and quasicrystals. *Key Eng. Mater*, 340–341, pp. 453–458. https://doi.org/10.4028/www.scientific.net/KEM.340-341.453
5. Zhou Y.-B., Li X.-F. (2018) Exact solution of two collinear cracks normal to the boundaries of a 1D layered hexagonal piezoelectric quasicrystal. *Philos. Mag*, 98, pp. 1780–1798. https://doi.org/10.1080/14786435.2018.1459057
6. Zhou Y. B.; Li X. F. (2018) Two collinear mode-III cracks in one-dimensional hexagonal piezoelectric quasicrystal strip. *Engineering Fracture Mechanics*, 189, pp. 133–147. https://doi.org/10.1016/j.engfracmech.2017.10.030
7. Tupholme G. E. (2018) A non-uniformly loaded anti-plane crack embedded in a half-space of a one-dimensional piezoelectric quasicrystal. *Meccanica*, 53, pp. 973–983. https://doi.org/10.1007/s11012-017-0759-1
8. Kletskov O. M., Silich-Balhabaieva V. B., Sheveleva A. E., Loboda V. V. (2025) On deformation peculiarities of two thin strips with a microcrack at the interface. *Scientific Journal of TNTU*, 118 (2), pp. 153–167. https://doi.org/10.33108/visnyk_tntu2025.02.153
9. Hu K. Q., Jin H., Yang Z., Chen X. (2019) Interface crack between dissimilar one-dimensional hexagonal quasicrystals with piezoelectric effect. *Acta Mech*, 230, pp. 2455–2474. https://doi.org/10.1007/s00707-019-02404-z
10. Govorukha V., Kamlah M. (2024) Interface crack with mixed electric boundary conditions in quasicrystals. *Arch. Appl. Mech*, 94, pp. 589–607. https://doi.org/10.1007/s00419-024-02538-0
11. Loboda V., Sheveleva A., Komarov O., Chapelle F., Lapusta Y. (2022) Arbitrary number of electrically permeable cracks on the interface between two one-dimensional piezoelectric quasicrystals with piezoelectric effect. *Eng. Fract. Mech*, 276 pp. 108878. https://doi.org/10.1016/j.engfracmech.2022.108878
12. Hao T. H., Shen Z. Y. (1994) A new electric boundary condition of electric fracture mechanics and its applications. *Eng. Fract. Mech*, 47, pp. 793–802. https://doi.org/10.1016/0013-7944(94)90059-0
13. Yang J., Li X. (2014) The anti-plane shear problem of two symmetric cracks originating from an elliptical hole in 1D hexagonal piezoelectric QCs. *Adv. Mater. Res*, 936, pp. 127–135. https://doi.org/10.4028/www.scientific.net/AMR.936.127
14. Muskhelishvili N. I. (1975). *Some Basic Problems of the Mathematical Theory of Elasticity.* Noordhoff, Groningen.
15. Zhou Y.-B., Li X.-F. (2018) Exact solution of two collinear cracks normal to the boundaries of a 1D layered hexagonal piezoelectric quasicrystal. *Philos. Mag*, 98, pp. 1780–1798. https://doi.org/10.1080/14786435.2018.1459057
16. Li X. Y., Li P. D., Wu T. H. (2014) Three-dimensional fundamental solutions for one-dimensional hexagonal quasicrystal with piezoelectric effect. *Phys. Lett. A*, 378, pp. 826–834. https://doi.org/10.1016/j.physleta.2014.01.016

УДК 539.3

МІЖФАЗНА ТРІЩИНА В 1Д П'ЄЗОЕЛЕКТРИЧНОГО КВАЗІКРИСТАЛУ ПІД ДІЄЮ АНТИПЛОСКОГО МЕХАНІЧНОГО НАВАНТАЖЕННЯ ТА ЕЛЕКТРИЧНОГО ПОЛЯ

Мухамед Альтумаймі; Володимир Лобода

Дніпровський національний університет імені Олеся Гончара, Дніпро, Україна

Резюме. *Розглянуто тріщину типу III на межі розділу двох одновимірних квазікристалів з п'єзоелектричним ефектом під дією антиплоского фазонного і фононного механічного навантаження та плоского електричного навантаження в площині, що аналізується. Використанио метод комплексних потенціалів. Усі електромеханічні параметри представлені через вектор-функції, аналітичні на всій комплексній площині, крім області тріщини. Для аналізу в якості основних прийнято моделі електрично непроникної тріщини та тріщини зі скінченною електричною проникністю. Перший випадок призводить до векторної задачі Гільберта з відповідною умовою на нескінченності, а другий додатково вимагає розв'язання квадратного рівняння відносно електричного потоку через область тріщини. Окремо розглянуто також випадок ненульового електричного зміщення, заданого на берегах тріщини. Для всіх проаналізованих видів електричних умов на берегах тріщини знайдено аналітичні формули для фононних і фазонних напружень та стрибків переміщень, а також для електричних складових уздовж межі розділу матеріалів. Крім того, отримано аналітичні формули для відповідних коефіцієнтів інтенсивності напружень у вершинах тріщини. Для числової ілюстрації обрано три варіанти навантаження, що включали різні значення фононного та фазонного напружень і електричного зміщення, заданих на віддаленні від тріщини. Для кожного з вказаних варіантів знай-дено відповідні значення електричного потоку через область тріщини. Інші числові результати представлено у графічному й табличному вигляді. Зокрема, представлено графіки зміни фононного і фазонного зсувного напружень та електричного зміщення вздовж правого продовження тріщини. Крім того, наведено також варіації фононних та фазонних стрибків зміщень берегів тріщини і стрибок електричного потенціалу в області тріщини. На основі аналізу аналітичних та чисельних результатів зроблено висновки стосовно якісних особливостей деформування п'єзоелектричного квазікристалічного композиту із тріщиною типу III на межі поділу матеріалів.*

Ключові слова: *міжфазна тріщина, напруження, квазікристал, антиплоске навантаження, обмежена електрична проникність, задача лінійного спряження.*

https://doi.org/10.33108/visnyk_tntu2025.03.012 *Отримано 11.08.2025*